

197549  
P-4

## Surface-Induced Brightness Temperature Variations and Their Effects on Detecting Thin Cirrus Clouds Using IR Emission Channels in the 8-12 $\mu\text{m}$ Region

N94-22341

Bo-Cai Gao, and W. J. Wiscombe

Climate & Radiation Branch, Code 913, NASA Goddard Space Flight Center  
Greenbelt, MD 20771

### Abstract

A method for detecting cirrus clouds in terms of brightness temperature differences between narrow bands at 8, 11, and 12  $\mu\text{m}$  has been proposed by Ackerman et al. (1990). In this method, the variation of emissivity with wavelength for different surface targets was not taken into consideration. Based on state-of-the-art laboratory measurements of reflectance spectra of terrestrial materials by Salisbury and D'Aria (1992), we have found that the brightness temperature differences between the 8 and 11  $\mu\text{m}$  bands for soils, rocks and minerals, and dry vegetation can vary between approximately  $-8$  K and  $+8$  K due solely to surface emissivity variations. We conclude that although the method of Ackerman et al. is useful for detecting cirrus clouds over areas covered by green vegetation, water, and ice, it is less effective for detecting cirrus clouds over areas covered by bare soils, rocks and minerals, and dry vegetation. In addition, we recommend that in future the variation of surface emissivity with wavelength should be taken into account in algorithms for retrieving surface temperatures and low-level atmospheric temperature and water vapor profiles.

### 1. Introduction

Thin cirrus clouds partially scatter solar radiation back to space and partially prevent the escape to space of the longwave emission originating from the surface and lower atmosphere. They are difficult to detect in images taken from current satellite platforms. The NASA FIRE Cirrus Program (Starr, 1987) was designed to improve our understanding of physical and radiative properties of cirrus clouds and their effects on the climate system.

Ackerman et al. (1990) developed a method for detecting thin cirrus clouds using three narrow channels at 8 (8.3-8.4), 11 (11.06-11.25), and 12

(11.93-12.06)  $\mu\text{m}$ . The method, referred to as the '8-11-12  $\mu\text{m}$  method' hereinafter, was based on the analysis of data acquired with the Cloud and Aerosol Lidar (CALs) (Spinhirne and Hart, 1990) and the High-spectral resolution Interferometer Sounder (HIS) (Revercomb et al., 1988) on board an ER-2 aircraft over areas covered by vegetation and water in Wisconsin during the first FIRE Cirrus Field Experiment in October 1986. Figure 1 illustrates the method (Ackerman et al., 1990). Basically, the cloud-free regions have negative brightness temperature differences between the 8 and 11  $\mu\text{m}$  channels ( $\Delta$  BT (8 - 11)) while the areas covered by cirrus clouds have positive brightness temperature differences ( $> 1$  K). The additional use of brightness temperature differences between the 11 and 12  $\mu\text{m}$  channels,  $\Delta$  BT (11 - 12), is for the purpose of separating the cirrus clouds from the low level water clouds. When applying the 8-11-12  $\mu\text{m}$  method to a similarly measured data set but over a different geographic location, the method failed to detect thin cirrus clouds (S. A. Ackerman, personal communication, 1992).

During their development of the 8-11-12  $\mu\text{m}$  method, Ackerman et al. (1990) carefully considered the absorption and scattering properties of water and ice particles, and the absorption and emission effects of atmospheric water vapor. The variation of surface emissivity with wavelength was not taken into consideration, however.

Recently, Salisbury and D'Aria (1992) have made state-of-the-art laboratory measurements of reflectance spectra of terrestrial materials between 2 and 14  $\mu\text{m}$ . We have studied surface-induced brightness temperature variations in the 8-14  $\mu\text{m}$  region using these spectra. Some of our findings relevant to remote sensing of cirrus clouds are presented in this paper.

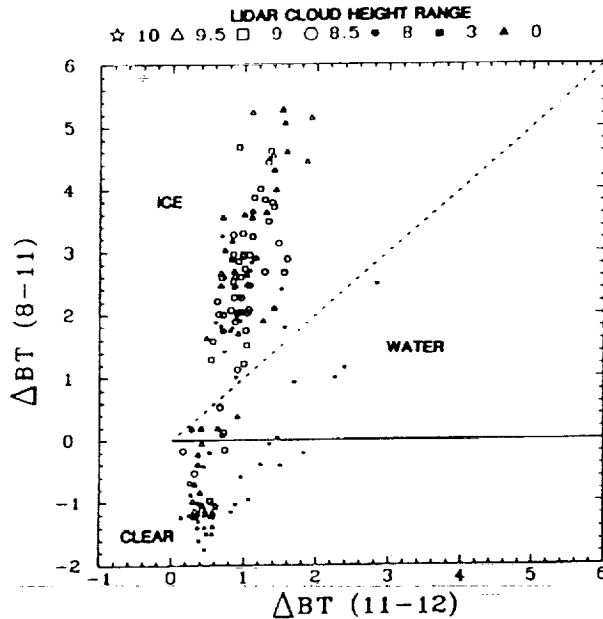


Fig. 1: Scatter diagram of  $\Delta BT (8 - 11)$  versus  $\Delta BT (11 - 12)$  (Ackerman et al., 1990). Each symbol represents a range in cloud altitude determined with the Cloud and Aerosol Lidar (CALs) (Spinhirne and Hart, 1990).

## 2. Surface Reflectance Spectra

Directional hemispherical reflectance spectra of a variety of rocks and minerals, soils, green and dead vegetation, water and ice have been made and summarized by Salisbury and D'Aria (1992). They were measured using Fourier transform spectrometers with integration sphere attachments. Figure 2 shows examples of reflectance spectra of three types of rocks; various absorption features due to vibrational band transitions can be seen. The reflectances in the 11 (11.06-11.25)  $\mu\text{m}$  region for ijolite and limestone are greater than those in the 8 (8.3-8.4)  $\mu\text{m}$  region, while the converse is true for sandstone. Figure 3 shows examples of reflectance spectra of three types of soils; various absorption features can be seen. Figure 4 shows sample reflectance spectra of green and dry vegetation. The green vegetation has nearly a constant reflectance value (0.02) in the 8-14  $\mu\text{m}$  region, while the dry vegetation has several absorption bands.

Figure 5 shows sample reflectance spectra of sea water and sea ice (rough surface); the

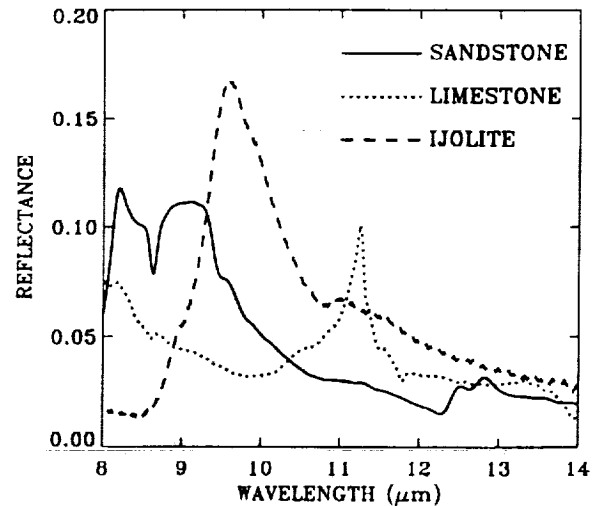


Fig. 2: Examples of reflectance spectra of three types of soils (Salisbury and D'Aria, 1992).

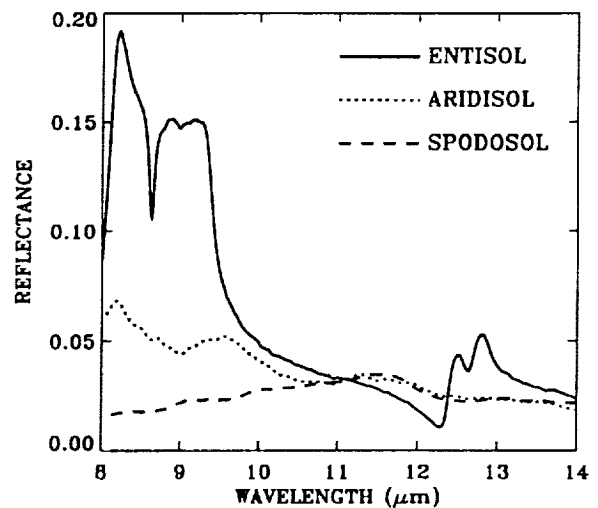


Fig. 3: Examples of reflectance spectra of three types of soils (Salisbury and D'Aria, 1992).

reflectances are small (between approximately 0.01 and 0.04). The reflectance minimum for sea water is located near 11  $\mu\text{m}$ , that for sea ice near 10.3  $\mu\text{m}$ . The emissivity is defined as one minus reflectance. It is easy to see from Figures 2, 3, 4, and 5 that the emissivities for soils, rocks and minerals, and dry vegetation in the 8-14  $\mu\text{m}$  region vary significantly with wavelength. The emissivities for green vegetation, water, and ice do not vary much with wavelength and are generally greater than 0.96.

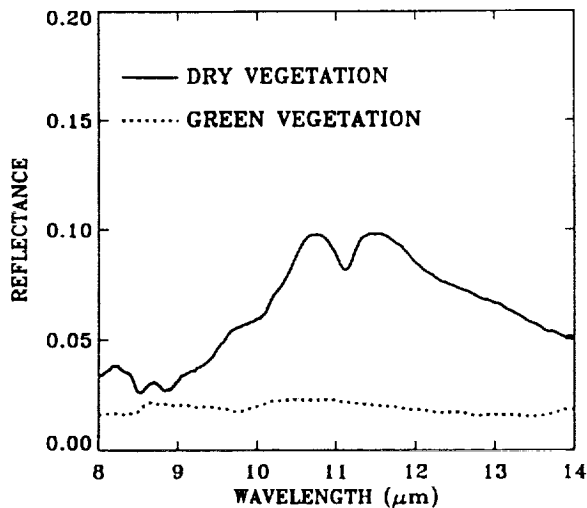


Fig. 4: Examples of reflectance spectra of dry and green vegetation (Salisbury and D'Aria, 1992).

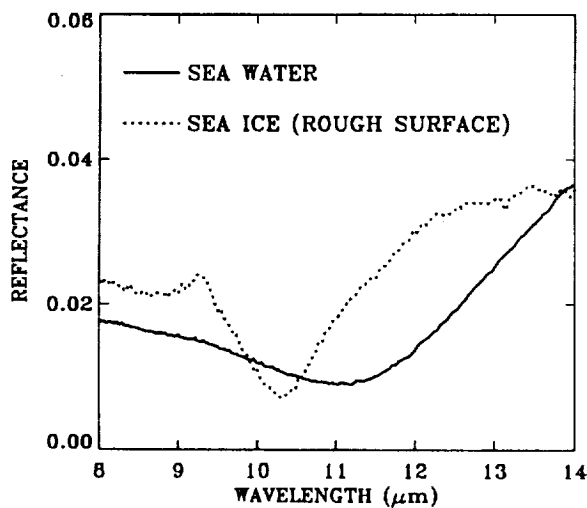


Fig. 5: Examples of reflectance spectra of sea water and ice (Salisbury and D'Aria, 1992).

### 3. Sensitivity of Brightness Temperature to Emissivity

The brightness temperature of a surface is a function of both its kinetic temperature and emissivity. We have studied the sensitivity of the Planck function to changes in temperatures for surface temperatures of 270, 280, 290, and 300 K. From these sensitivities, we have derived the sensitivities of brightness temperatures to emissivities. The results show that, for kinetic temperatures between 270 and 300 K, an error of 0.01 in assumed surface emissivity results in errors

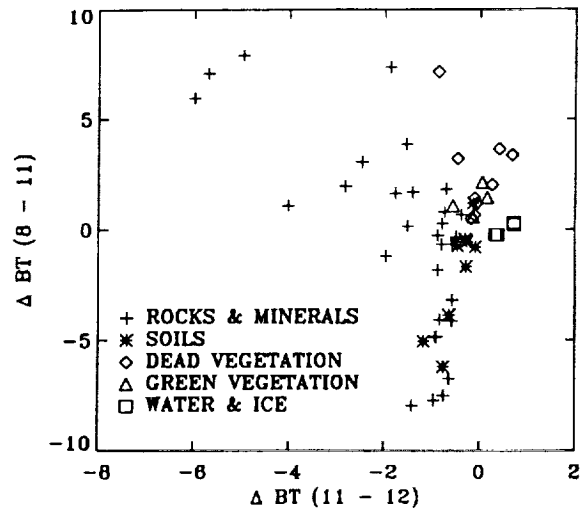


Fig. 6: Scatter diagram of surface-induced  $\Delta BT$  (8 - 11) versus  $\Delta BT$  (11 - 12) for rocks and minerals, soils, dead and green vegetation, and water and ice (rough surface).

of approximately 0.48 K in surface temperature at 8.35  $\mu\text{m}$ , 0.63 K at 11.155  $\mu\text{m}$ , and 0.67 K at 11.995  $\mu\text{m}$ .

### 4. Results

Based on the sensitivity of brightness temperatures to surface emissivity described in Section 3 and using the reflectance data from Salisbury and D'Aria (1992), we have quantified the surface-induced brightness temperature variations in the 8, 11, and 12  $\mu\text{m}$  region for soils, rocks and minerals, green and dry vegetation, and water and ice. Figure 6 shows the scatter diagram of the  $\Delta BT$  (8 - 11) versus  $\Delta BT$  (11 - 12). The surface-induced  $\Delta BT$  (8 - 11) can vary between approximately -8 K and 8 K for rocks and minerals, 0.5 to 7 K for dead vegetation, -6 and 1 K for soils. These differences are greater than the  $\Delta BT$  (8 - 11) in Figure 1.

The large differences in the surface-induced  $\Delta BT$  (8 - 11) are sufficient to cause confusion when using the 8-11-12  $\mu\text{m}$  method for detecting cirrus clouds. For example, if the measurements were made from high-altitude aircraft or satellite platforms over areas covered by dead vegetation but no cirrus clouds, the straight forward application of the 8-11-12  $\mu\text{m}$  method would misidentify the areas as being covered by cirrus clouds. On the other hand, if the same

measurements were made over areas covered by bare soils with a -4 K surface-induced  $\Delta BT$  (8 - 11) and also covered by very thin cirrus clouds with a 1 K cirrus-induced  $\Delta BT$  (8 - 11), the application of the 8-11-12  $\mu m$  method would identify the areas as being clear.

### 5. Discussion

Because of the traditional lack of reliable IR emissivity measurements (Salisbury and D'Aria, 1992) of terrestrial materials, algorithms developed for retrieving atmospheric temperatures and surface temperatures from satellite IR emission channels typically assume constant values of emissivity (about 0.96) in the 8-14  $\mu m$  spectral region. As a result, errors of 10 K or greater in the derived surface temperatures from current satellite IR emission measurements exist (Wu and Chang, 1991).

### 6. Summary

We have studied surface-induced brightness temperature variations in the 8-12  $\mu m$  spectral region using laboratory measurements of emissivity of terrestrial materials (Salisbury and D'Aria, 1992). It is found that the brightness temperature differences between the 8 and 11  $\mu m$  bands for soils, rocks and minerals, and dry vegetation can vary between approximately -8 K and 8 K. We conclude that although the 8-11-12  $\mu m$  method of Ackerman et al. (1990) is useful for detecting cirrus clouds over areas covered by green vegetation, water, and ice, the technique is less effective for detecting cirrus clouds over areas covered by bare soils, rocks and minerals, and dry vegetation. We suggest that the variation of surface emissivity with wavelength should also be taken into account in algorithms for retrieving surface temperatures and low-level atmospheric temperature and water vapor profiles.

### 7. Acknowledgments

The authors are grateful to J. W. Salisbury at the Department of Earth and Planetary Sciences, Johns Hopkins University for providing the emissivity spectra of terrestrial materials in digital form. This research was partially supported by the NASA FIRE Project Office through a grant to the NASA Goddard Space Flight Center.

### 8. References

- Ackerman, S., W. L. Smith, J. Spinhirne, and H. Revercomb, The 27-28 October FIRE IFO cirrus case study: Spectral properties of cirrus clouds in the 8-12  $\mu m$  window, *Mon. Wea. Rev.*, 118, 2377-2388, 1990.
- Revercomb, H., H. Buijs, H. Howell, D. LaPorte, W. L. Smith, and L. Sromovsky, Radiometric calibration of IR Fourier transform spectrometer: Solution to a problem with the High-spectral resolution Interferometer Sounder, *Appl. Opt.*, 27, 3210-3218, 1988.
- Salisbury, J., and D. D'Aria, Emissivity of terrestrial materials in the 8-14  $\mu m$  atmospheric window, *Remote Sens. Env.*, 42, 83-106, 1992.
- Spinhirne, J., and W. Hart, The 27-28 October 1986 FIRE cirrus case study: ER-2 lidar and spectral radiometer cirrus observations, *Mon. Wea. Rev.*, 118, 2329-2343, 1990.
- Starr, D., A cirrus cloud experiment: Intensive field observations planned for FIRE, *Bull. Amer. Meteor. Soc.*, 67, 119-124, 1987.
- Wu, M.-L., and L. Chang, Differences in global data sets of atmospheric and surface parameters and their impact on outgoing longwave radiation and surface downward flux calculations, *J. Geophys. Res.*, 96, 9227-9262, 1991.